Morpholino Spin-Labeling for Base-Pair Sequencing of a 3′-Terminal RNA Stem by Proton Homonuclear Overhauser Enhancements: Yeast Ribosomal 5S RNA†

Kai Mon Lee‡ and Alan G. Marshall*,§
Department of Biochemistry, The Ohio State University, Columbus, Ohio 43210
Received October 20, 1986; Revised Manuscript Received March 31, 1987

ABSTRACT: Base-pair sequences for 5S and 5.8S RNAs are not readily extracted from proton homonuclear nuclear Overhauser enhancement (NOE) connectivity experiments alone, due to extensive peak overlap in the downfield (11–15 ppm) proton NMR spectrum. In this paper, we introduce a new method for base-pair proton peak assignment for ribosomal RNAs, based upon the distance-dependent broadening of the resonances of base-pair protons spatially proximal to a paramagnetic group. Introduction of a nitroxide spin-label covalently attached to the 3′-terminal ribose provides an unequivocal starting point for base-pair hydrogen-bond proton NMR assignment. Subsequent NOE connectivities then establish the base-pair sequence for the terminal stem of a 5S RNA. Periodate oxidation of yeast 5S RNA, followed by reaction with 4-amino-2,2,6,6-tetramethylpiperidinyl-1-oxy (TEMPO-NH_2) and sodium borohydride reduction, produces yeast 5S RNA specifically labeled with a paramagnetic nitroxide group at the 3′-terminal ribose. Comparison of the 500-MHz ^1H NMR spectra of native and 3′-terminal spin-labeled yeast 5S RNA serves to identify the terminal base pair (G_1·C_{120}) and its adjacent base pair (G_2·U_{119}) on the basis of their proximity to the 3′-terminal spin-label. From that starting point, we have then identified (G·C, A·U, or G·U) and sequenced eight of the nine base pairs in the terminal helix via primary and secondary NOE's.

Proton homonuclear Overhauser enhancement (NOE) experiments have successfully *identified* (i.e., G·C, A·U, G·U) and *assigned* (to specific primary sequence bases) almost all of the secondary (and tertiary) base pairs in several transfer ribonucleic acids in aqueous solution (Heerschap et al., 1982, 1983a,b; Hare & Reid, 1982a,b; Roy & Redfield, 1983; Johnston & Redfield, 1981; Reid, 1981; Schimmel & Redfield, 1980). A sufficient number of such assignments serves to determine the secondary structure of tRNA in solution.

However, extension of this direct and powerful nuclear magnetic resonance (NMR) technique to the determination of base-pair sequences in the larger 5S RNA in solution presents several major problems. First, the three-dimensional structure of crystalline $tRNA^{Phe}$ (Rich, 1977; Kim, 1976) was known in advance of the NMR studies of tRNA solution structure. To be fair, proton NMR was then used to determine the secondary structures of many other tRNAs in advance of their crystal structures. Although single crystals of 5S rRNA have been reported, the crystals have so far been of insufficient quality to yield useful structural information (Abdel-Meguid et al., 1983; Morikawa et al., 1982). Second, there are ~120 base pairs in 5S rRNA against ~80 base pairs in a typical tRNA, resulting in greater overlap of base-pair hydrogen-bond imino proton resonances in the region 9–15 ppm downfield from tetramethylsilane. Third, the higher molecular weight of 5S rRNA leads to broader ^1H NMR resonances (exacerbating peak overlap) and longer longitudinal magnetic relaxation times, T_1 (requiring a longer data acquisition period).

Strategies applied to RNA NMR spectral assignments include ring current prediction (Arter & Schmidt, 1976; Hurd & Reid, 1979a,b; Shulman et al., 1973); isolation of enzymatic cleavage fragments (Boyle et al., 1980; Kime & Moore, 1983; Kime et al., 1984; Li & Marshall, 1986; Chen & Marshall, 1986; Li et al., 1987); spectral comparisons between RNAs of similar primary sequence (Rordorf et al., 1976; Hurd & Reid, 1979a; Chen & Marshall 1986); proton homonuclear NOE's; and change in salt concentration or temperature to induce differential shifts or intensity changes in selected resonances (Heerschap et al., 1982, 1983a,b; Kime & Moore, 1983; Li & Marshall, 1986; Lee & Marshall, 1986a; Lee, 1986).

Semiempirical ring current calculations have proved quite helpful in accounting for the chemical shifts of base-pair imino proton resonances in tRNA (e.g., $tRNA^{Phe}$; Johnston & Redfield, 1981) but not for 5S rRNA for several reasons. First, all RNA helices are assumed to have the same conformation (A helix) in the ring current calculations. This assumption holds quite well for tRNAs as confirmed by their three-dimensional structure. For 5S RNA, however, the extent of secondary A-helix conformation is not known; the tertiary conformation is not known; and G·U base pairs, which are common in 5S rRNA (Chang & Marshall, 1983), are rare in tRNA. Moreover, the chemical shift induced by a G·U base pair upon other base-pair hydrogen-bond imino protons is not well understood. The idea of treating a G·U pair as if it were a G·C pair for purposes of ring current effects (Reid et al., 1979; Johnston & Redfield, 1981) is questionable, because the three-dimensional structure of $tRNA^{Phe}$ reveals that a G·U pair can distort the RNA from its basic A-helix conformation (Mizuno & Sundaralingam, 1978).

Proton NMR characterization of purified RNA fragments obtained via specific enzymatic cleavage (Kime & Moore, 1983; Kime et al., 1984; Li & Marshall, 1986; Chen & Marshall, 1986) offers a promising approach, provided that the fragments retain the structure of the intact 5S rRNA molecule. Differential temperature-induced chemical shifts have been exploited successfully by Lee and Marshall (1986a) to demonstrate the existence of the exceptionally thermally stable common G·C-rich arm in yeast 5.8S rRNA. The use of stepwise temperature-induced melting to assign resonances

† Supported by grants (A.G.M.) from the U.S. Public Health Service (NIH 1 R01 GM-29274; NIH 1 S10 RR-01458) and The Ohio State University.
‡ Present address: St. Luke's-Roosevelt Hospital Center, Columbia University, New York, NY 10025.
§ Also a member of the Department of Chemistry.

0006-2960/87/0426-5534$01.50/0

in 5S rRNA is rendered difficult by the apparent lack of any uniquely thermally stable helical secondary-structural segment.

In this paper, we apply an alternative technique designed to complement proton NOE's for base-pair sequencing in RNA. The method begins by attaching covalently a paramagnetic nitroxide spin label at a specific site on the RNA molecule. The strong electron magnetic moment will then dipolar relax any protons that are spatially near (<15 Å) the nitroxide group, according to an inverse sixth-power distance dependence. Thus, the proton NMR signals from the hydrogen-bond imino protons in base pairs closest to the spin-labeled site will exhibit the largest peak broadening and can readily be identified to give a starting point for base-pair sequencing. The method is demonstrated by introducing the morpholino spin-label (4-amino-2,2,6,6-tetramethylpiperidinyl-1-oxy, also known as TEMPO-NH_2) to the UCUA 3′-terminus of the yeast 5S rRNA molecule. Spin-label-assisted assignment of the two most terminal base pairs can then be combined with homonuclear NOE's to assign and sequence successively most of the remaining base pairs of the RNA terminal helix.

Materials and Methods

Isolation and Purification of Yeast 5S rRNA. Brewers' yeast (*Saccharomyces carlsbergensis*) cells were generously provided by the Annheuser-Busch Brewery, Inc., Columbus, OH. The isolation and purification procedure has been described by Lee and Marshall (1986b). 5S rRNA was extracted from the cells according to the procedure of Rubin (1975). Specifically, yeast cells were suspended in a buffer containing 20 mM EDTA, 0.1 M sodium acetate, and 1% sodium dodecyl sulfate (SDS), pH 5.0. One-half volume of phenol was added and the mixture stirred vigorously for 2 h at room temperature. The phases were separated by centrifugation at 9800*g*, and the aqueous phase was removed and reextracted with an equal volume of phenol. RNA was then allowed to precipitate overnight at −20 °C after addition of 2.5 volumes of 95% ethanol. The precipitated RNA consisted of tRNAs, 5S rRNA, 5.8S rRNA, and other large rRNAs. Purification via ion-exchange (DEAE-32) and gel filtration (Sephadex G-75) chromatography yielded 5S rRNA of purity >92% as determined from 10% acrylamide gel electrophoresis.

Spin-Labeling of Yeast 5S rRNA with TEMPO-NH_2 (Morpholino Spin-Label). Yeast 5S rRNA was spin-labeled with 4-amino-2,2,6,6-tetramethylpiperidinyl-1-oxy (TEMPO-NH_2) according to the modified procedure described for tRNA by Caron and Dugas (1976). TEMPO-NH_2 was purchased from Eastman Kodak, Rochester, NY. The reaction is shown in Figure 1. About 40 mg of pure yeast 5S rRNA was dissolved in 6 mL of a 1.0 M sodium acetate buffer (pH 5.0) containing 20 mM sodium periodate to generate a terminal dialdehyde RNA species. This method was shown to be specific for the labeling of the 1′,2′-diol end group in RNA (Caron & Dugas, 1976; Hansske et al., 1974; Ofengand & Chen, 1972; RajBhandary, 1968; Cramer et al., 1968). The solution was stirred at 4 °C for 2 h in the dark, then neutralized by addition of sodium hydroxide, and precipitated with cold ethanol. The precipitated dialdehyde RNA species was washed with acetone and carefully dried with nitrogen.

The precipitate was dissolved in 5.5 mL of 0.2 M sodium bicarbonate buffer (pH 9.5) containing 10% dimethyl sulfoxide, and 45 mg of TEMPO-NH_2 was slowly added. The solution was stirred at 0 °C in dark for 90 min. The amine functionality of TEMPO-NH_2 reacts with the aldehyde groups via a Schiff base reaction, thereby generating an imine. The imine was then reduced and ring closed via the addition of 0.23

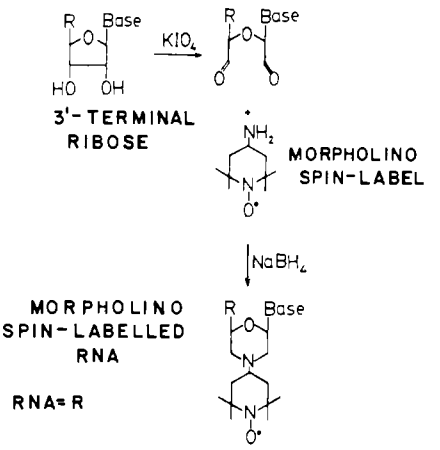

FIGURE 1: Chemical reaction scheme for spin-labeling of yeast 5S rRNA with a paramagnetic morpholino spin-label (TEMPO-NH_2).

mL of freshly prepared 0.6 M sodium borohydride ($NaBH_4$) solution. The solution was stirred for 30 min, after which another 0.23 mL of the $NaBH_4$ solution was added and the solution stirred for an additional 30 min. The mixture was then exhaustively dialyzed against 10 mM Tris buffer (pH 7.0) containing 100 mM sodium chloride with five buffer changes. The spin-labeled yeast 5S rRNA was next dialyzed against 10 mM Tris buffer (pH 7.0) containing 10 mM EDTA and 100 mM sodium chloride and finally against the same buffer but containing 1 mM EDTA.

NMR Samples. The dialyzed nitroxide spin-labeled yeast 5S rRNA in 10 mM Tris buffer (pH 7.0) containing 100 mM NaCl and 1 mM EDTA was concentrated via AMICON Centricon 10 micro-concentrator (AMICON Corp., Danvers, MA) to give a final concentration of 34 mg/mL. D_2O was added to give a final 5% D_2O concentration to provide a deuterium field-frequency lock signal. Gel electrophoresis on the nitroxide-labeled yeast 5S rRNA showed that the 5S RNA was not fragmented by the spin-labeling procedure.

EPR Spectroscopy. Electron paramagnetic resonance spectra were recorded on a Varian E-4 EPR spectrometr operating at 9.5 GHz.

Proton NMR and NOE Spectroscopy. All proton NMR spectra were obtained with a Bruker AM-500 FT/NMR spectrometer, with phase-cycled quadrature detection. Chemical shifts were measured relative to H_2O and referred to DSS [3-(trimethylsilyl)-1-propanesulfonic acid] from an independent calibration. Water suppression was achieved via a 1331-hard-pulse sequence (Hore, 1983) with the radiofrequency carrier centered at the water resonance. Alternatively, NOE difference spectra were produced via a modified Redfield 21412-pulse sequence (Redfield et al., 1975; Chang & Marshall, 1986) with the radiofrequency carrier located at 15 ppm (i.e., 5100 Hz away from the water resonance). An acquisition period of 100 ms (4K time domain data) and a relaxation delay of 0.5 s were typical. With either excitation, the final spectrum gave a base line that required only slight flattening.

NOE difference spectra were obtained at relatively low decoupler power (0.2–0.5 mW, corresponding to a bandwidth of 15.3–21.4 Hz) for selective saturation (preirradiation period 0.6 s, to prevent extensive spin diffusion) of the resonance of interest, with off-resonance irradiation at 18 ppm. NOE difference spectra were apodized to give a line broadening of 10 Hz in order to enhance the signal-to-noise ratio. In some cases NOE difference spectra were subjected to exponentially time-weighted resolution enhancement to resolve components of a multipeak envelope. Unless otherwise stated, NOE experiments were conducted at relatively low temperature (22

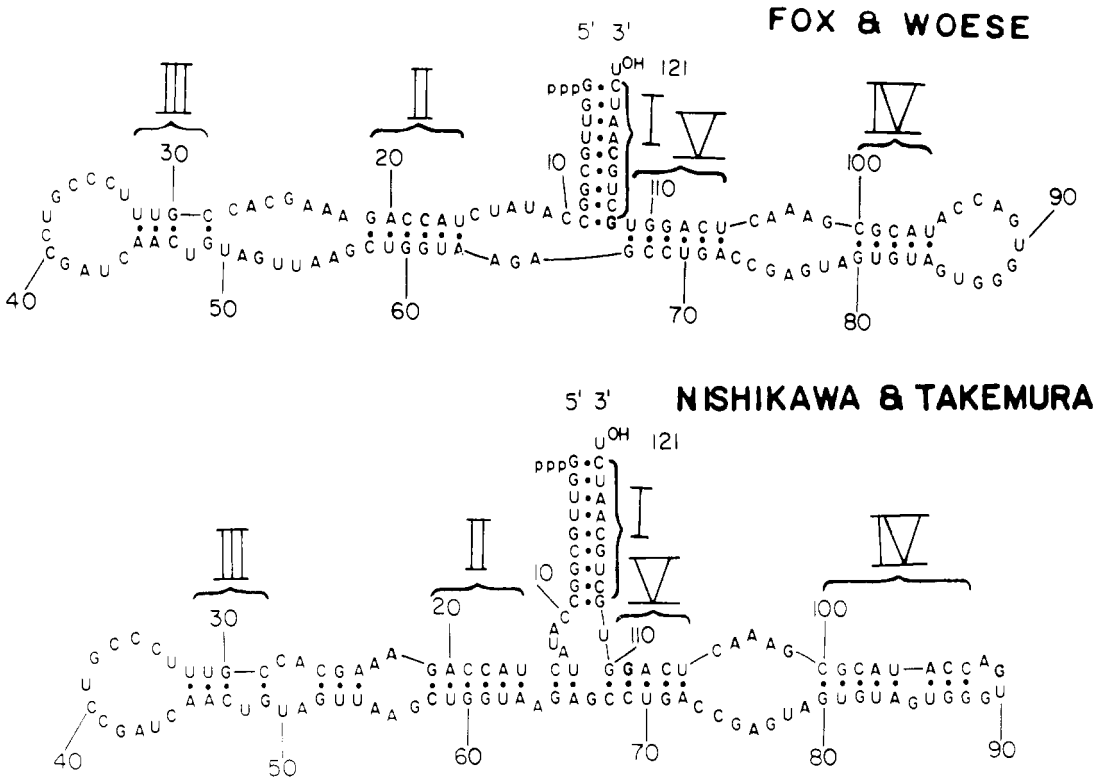

FIGURE 2: Two proposed secondary base-pairing schemes for 5S rRNA, each adapted to the primary sequence for *S. carlbergensis*.

°C) in order to prevent too rapid chemical exchange of hydrogen-bond imino protons with water protons.

Results and Discussion

Figire 2 shows two proposed 5S ribosomal RNA secondary base-pairing schemes (Fox & Woese, 1975; Nishikawa & Takemura, 1974a–c), adapted to the primary nucleotide sequence of *S. carlsbergensis*. Note that the terminal helix is the same for the Fox and Woese and the Nishikawa and Takemura models. Although four G·U's (three of which are the same) are proposed in both the Fox and Woese and the Nishikawa and Takemura models, the fourth G·U is assigned to a different base pair in the two cases. Thus, our first goal in NMR-based RNA base-pair sequence analysis is to identify and locate all of the G·U base pairs, as a sufficient condition for discriminating between the proposed 5S rRNA secondary structures. Since two G·U pairs are found in the terminal helix of both proposed models, correct identification and assignment of the terminal helix base pairs is crucial to the establishment of the correct secondary structure of yeast 5S RNA.

Yeast 5S RNA Does Not Possess a Uniquely Heat-Stable Secondary-Structural Segment. On the basis of a combination of proton homonuclear Overhauser enhancements and temperature dependence of the proton 500-MHz spectrum, we were able to identify and assign eight of the nine base pairs in the most thermally stable helical arm (rich in G·C pairs) of yeast 5.8S rRNA (Lee & Marshall, 1986a). However, it is obvious from Figure 2 that none of the proposed secondary helices of yeast 5S rRNA contain an extended sequence of consecutive G·C base pairs. Moreover, we present in Table I the free energy values computed from Tinoco stability rules (Gralla & Crothers, 1973) for each of the helical arms of the two structural models of Figure 2. Although Table I shows that helix I (i.e., the thermal helical stem) is the most thermally stable, none of the proposed secondary-structural segments exhibits the uniquely high thermal stability seen for the G·C-rich arm in 5.8S rRNA.

Table I: Free Energies of Stability for Individual Helices Computed from Tinoco Rules[a] for Two Proposed Secondary Structures of Yeast 5S Ribosomal RNA

helix	ΔG (kcal/mol)
Fox and Woese Model (Luehrsen & Fox, 1981)	
I	−11.9
II and III	−5.2 (including hairpin loop, bulge, interior loop)
IV and V	−4.0 (including hairpin loop and interior loop)
Nishikawa and Takemura Model (1974a–c)	
I	−11.9
II and III	−5.4 (including hairpin loop, bulge, interior loops)
IV and V	−12.7 (including hairpin, bulge, interior loop)

[a] Gralla & Crothers, 1973.

Figure 3 shows proton NMR downfield-region spectra of yeast 5S RNA as a function of temperature. Although some A·U resonances (e.g., peak A) melt at relatively low temperature, all of the base-pair proton resonances have melted at ≥61 °C, and there is no temperature at which a single helical segment yields a highly resolved subspectrum, as was the case for the G·C-rich arm of yeast 5.8S RNA at 61 °C (Lee & Marshall, 1986a). Furthermore, the use of G·U pairs as a starting point for base-pair assignment works less well for yeast 5S RNA (Chen & Marshall, 1986) than for *Bacillus subtilis* 5S RNA, because of peak overlap. We therefore need a different approach for identifying and assigning base pairs in yeast 5S rRNA, as described below.

Identification of Terminal Base Pairs from Selective ^1H NMR Peak Broadening Induced by a Spin-Label on the 3′-Terminal Ribose. Site-specific labeling of yeast 5S RNA is confirmed by the EPR spectra shown in Figure 4. The free TEMPO-NH_2 spin label gives an EPR spectrum with three narrow peaks of nearly equal intensity (Figure 4, top), as expected for a rapidly tumbling nitroxide in solution. The EPR spectrum of yeast 5S rRNA spin-labeled at the 3′-terminus with TEMPO-NH_2 (Figure 4, bottom) is quite similar to previous EPR spectra for RNAs carrying a single spin-label (Luoma et al., 1982; Caron & Dugas, 1975; Yang & Soll,

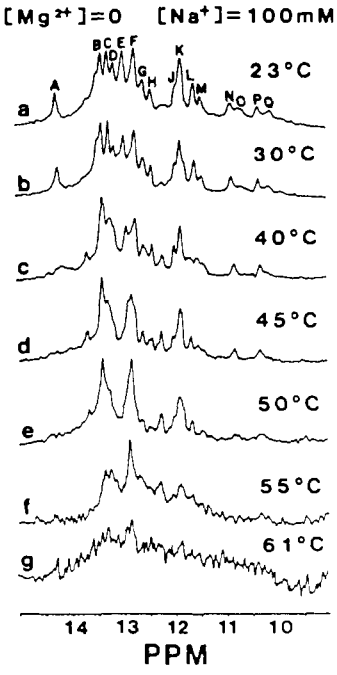

FIGURE 3: 500-MHz proton NMR spectra of yeast 5S rRNA at several temperatures.

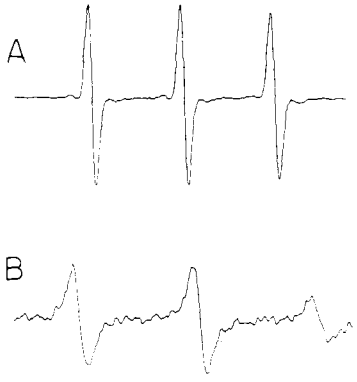

FIGURE 4: EPR spectra of the free morpholino spin-label (top) and spin-labeled yeast 5S rRNA (bottom).

1974). The shape of the spin-labeled RNA spectrum (Luoma et al., 1982) indicates that significant internal flexibility is present at the site of the spin-label attachment, as would be expected for labeling at the 3′-terminal ribose. It is worth noting that the EPR experiment detects only those RNA molecules that are spin-labeled and is blind to unlabeled RNA (see below).

Figure 5 shows the 500-MHz proton FT-NMR spectra of spin-labeled and native yeast 5S rRNA (ca. 34 mg/mL) in 10 mM cacodylate, 100 mM sodium chloride, 1 mM EDTA, pH 7.0, aqueous buffer, in the absence of Mg^{2+}. Comparison of the two spectra quickly reveals the largest reduction in intensity for the spin-labeled RNA at two spectral positions: namely, resonance F (12.74 ppm, corresponding to a typical G·C hydrogen-bond imino proton chemical shift) and resonance L (11.61 ppm, corresponding to a typical G·U hydrogen-bond imino proton chemical shift). The relative intensities in Figure 5 suggest that two base-pair hydrogen-bond imino protons contribute to peak L and three to peak F in native yeast 5S rRNA. Since 3′-terminal spin-labeling is expected to broaden the nearest base-pair protons below NMR observability, the reduction in intensity at peaks F and L in spin-labeled 5S rRNA is consistent with removal of at least 75% of one proton from the NMR spectrum. Thus, it may be concluded that the "spin-labeled" 5S RNA is indeed highly morpholino labeled at the 3′-terminus.

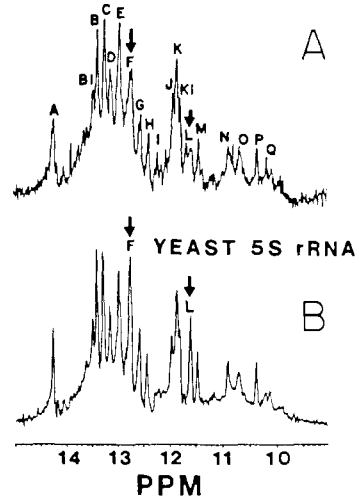

FIGURE 5: Proton 500-MHz FT-NMR spectra of yeast 5S rRNA in 10 mM Tris-HCl, pH 7.5, buffer containing 100 mM NaCl and 1 mM EDTA at room temperature: top, morpholino spin-labeled yeast 5S rRNA; bottom, unlabeled yeast 5S rRNA.

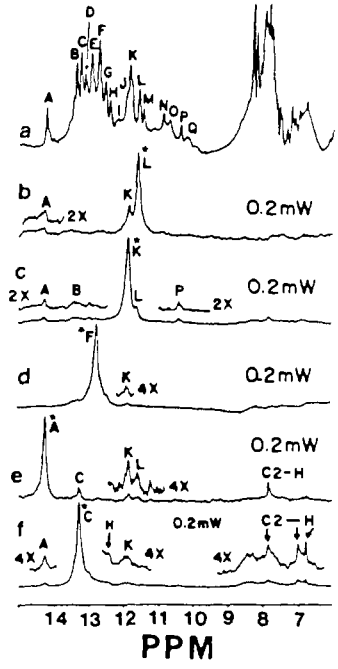

FIGURE 6: Proton 500-MHz FT-NMR spectrum (a) and proton homonuclear Overhauser difference spectra (b–f) resulting from irradiation of peaks L, K, F, A, and C at 22 °C. In each case, the irradiated peak is denoted by a star and decoupler power is shown at the right.

From the proposed models of Figure 2, it clear that resonances at F (12.74 ppm) and L (11.61 ppm) can immediately be assigned to $G_1 \cdot C_{120}$ and $G_2 \cdot U_{119}$ since only these two terminal base pairs are spatially close to the paramagnetic nitroxide spin-label chemically bound to the ribose of the unpaired U_{121} residue at the 3′-terminus of the RNA molecule. The small spin-label-induced intensity changes at peaks E, I, and possibly Q, if genuine, may represent tertiary folding, since those resonances do not arise from the 3′-terminal stem (Chen & Marshall, 1986).

Confirmation of the Assigned Terminal Base Pairs $G_1 \cdot C_{120}$ and $G_2 \cdot U_{119}$ by ^1H Homonuclear Overhauser Enhancements. NOE connectivity experiments may next be used to confirm the above assignments. The strong mutual NOE's observed

Table II: Assignments for Imino Proton Resonances from the Terminal Helix of Yeast 5S rRNA and Approximate (±5 °C) Temperatures for Onset of Melting (Judged from Proton NMR Spectrum)

resonance	chemical shift (ppm)	base pair	melting temp (°C)
F	−12.74	G_1·C_{120}	40
K/L	−11.85/11.61	G_2·U_{119}	40
A	−14.25	U_3·A_{118}	40
C	−13.28	U_4·A_{117}	40
H	−12.36	G_5·C_{116}	50
F	−12.74	C_6·G_{115}	50
K/P	−11.85/10.35	G_7·U_{114}	50
B	−13.38	G_8·C_{113}	*a*

[a] Although the component resonances from composite peaks F and K happen to melt at the common temperature, the component resonances of composite peak B do not.

via irradiation at peak L (11.61 ppm) and peak K (11.82 ppm) (Figure 6b,c) clearly confirm those two protons as arising from a G·U base pair. As noted previously for tRNAs and prokaryotic 5S RNA [see below and Chang and Marshall (1986)], K/L (a G·U pair) shows NOE connectivity to peak A (Figure 6b,c,e), but not to peak F (G_1·C_{120} see below). Peak A (14.25 ppm) is an A·U base pair, as seen from its narrow NOE difference peak at 7.77 ppm from an adenine C2-proton (Figure 6e). Thus, it may be concluded that peaks K/L are from a G·U pair adjacent to an A·U pair (peak A).

Irradiation at peak F (12.74 ppm, Figure 6d) shows a broad NOE in the aromatic region characteristic of a G·C pair, with weak NOE connectivity to peak K. At this stage, the base-pair sequence G·C (peak F)-G·U (peaks K/L)-A·U (peak A) could correspond either to C_{26}·C_{52}·G_{25}·U_{53}-A_{24}·U_{54} in helix III in the Nishikawa and Takemura model or to the G_1·C_{120}-G_2·U_{119}-U_3·A_{118} segment that is common to the terminal helix in both structural models (Figure 2). Thus, the NOE results alone cannot distinguish between these two possible assignments. However, since peaks F and L were selectively broadened by the 3′-terminal spin-label (Figure 5), it is clear that peak F must be G_1·C_{120} and peaks K/L must be G_2·U_{119} based upon their proximity to the paramagnetic morpholino label at U_{121}. The terminal helix base-pair sequence, F-K/L-A, may thus be assigned to G_1·C_{120}-G_2·U_{119}-U_3·A_{118}, as listed in Table II.

The present assignment of G_1·C_{120} to peak F (12.74 ppm) corrects a prior assignment by Chen and Marshall (1986) of base pair G_1·C_{120} as peak B (13.37 ppm). Because peaks K and F each contain more than one base-pair proton (thereby rendering NOE connnectivity conclusions ambiguous), the earlier assignment had to be based solely upon a low melting temperature of resonance B. In contrast, the present spin-label criterion offers unequivocal evidence for assignment of base pairs adjacent to the spin-label residue. Once a base pair has been unambiguously assigned, we may then proceed to sequence neighboring base pairs by NOE connectivity alone, as discussed below.

Base-Pair Sequencing of the Remaining Terminal Helix via Proton NOE Connectivities. Irradiation at peak K (11.85 ppm) produces strong mutual NOE's to peaks L (11.61 ppm) and P (10.35 ppm), as seen from Figure 6b,c and 7d,e. Thus, peak K must contain resonances from two different G·U base pairs (peaks K/L and K/P), as previously inferred for the 5S RNA of highly similar primary sequence from *Torulopsis utilis* (Chen & Marshall, 1986). The resolution-enhanced proton spectra in Figure 5 indeed show that resonance K is actually composed of two peaks (11.85, 11.80 ppm).

Proceeding further, the mutual weak NOE's between the A·U pairs corresponding to peaks A and C (Figure 6e,f) indicate their adjacent relationship. Irradiation at peak C (13.28 ppm) reveals that it contains three A·U as evident by the three narrow NOE peaks at 7.80, 6.97, and 6.75 ppm. One of these A·U pairs must lie between an A·U (peak A) and a G·C (peak H) (Figures 6e,f and 7b), because irradiation of either peak H (12.36 ppm) or peak A gives a strong NOE connectivity to peak C. Figure 7b shows that peak H is a G·C pair from the broad NOE difference spectrum at the aromatic region. [Minor variations in the appearance of the 6–9 ppm region in Figure 6 are typical of such NOE experiments and can arise from (e.g.) variation in decoupler power at the H_2O peak and variation in phasing between different experiments.] At this point, five out of nine base pairs in the sequence G·C(F)-G·U(K/L)-A·U(A)-A·U(C)-G·C(H), which corresponds to the segment G_1·C_{120}-G_2·U_{119}-U_3·A_{118}-U_4·A_{117}-G_5·C_{116} in the terminal helix, have been identified.

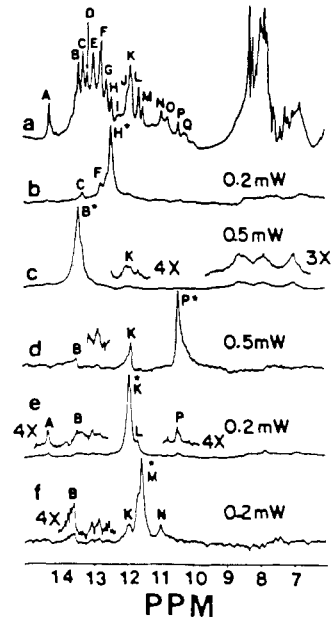

FIGURE 7: 500-MHz proton homonuclear Overhauser difference spectra of yeast 5S rRNA, produced as in Figure 6, for peaks H, B, P, K, and M.

Irradiation at peak H produces NOE connectivities to peaks F and C (Figure 7b). Since NOE connectivity (see above) shows that peaks K/P arise from a G·U base pair, which has been shown by means of enzymatic cleavage experiments to lie in the terminal helix (Chen & Marshall, 1986), peaks K/P must correspond to G_7·U_{114}. Irradiation at peak P also elicits a weak NOE connectivity to the G·C resonance at peak B (13.38 ppm) as shown in Figure 7c,d. Peak B could thus represent either C_6·G_{115} or G_8·C_{113}. However, since irradiation at peak H (G_5·C_{116}) produces a definite NOE at peak F (Figure 7b) and since peak F gives NOE behavior characteristic of a G·C base pair (Figure 6d), it is logical to assign peak C_6·C_{115} to peak F, leaving peak B as G_8·C_{113}. Although we cannot infer unambiguous base-pair sequences proceeding through peak F (because it contains more than one base-pair imino proton), we have already shown that another component of peak F is G_1·C_{120}.

Our sequence assignments can now be extended to include eight of the nine base pairs of the terminal helix (see Table II): G_1·C_{120}(F)-G_2·U_{119}(K/L)-U_3·A_{118}(A)-U_4·A_{117}(C)-G_5·C_{116}(H)-C_6·G_{115}(F)-G_7·U_{114}(K/P)-G_8·C_{113}(B). The terminal ninth base pair of the helix remains unidentifiable via NOE's, perhaps due to its presumably higher exchange rate with the solvent.

Identification of G·U Base Pairs. As noted above, G·U imino resonances form an excellent starting point for base-pair

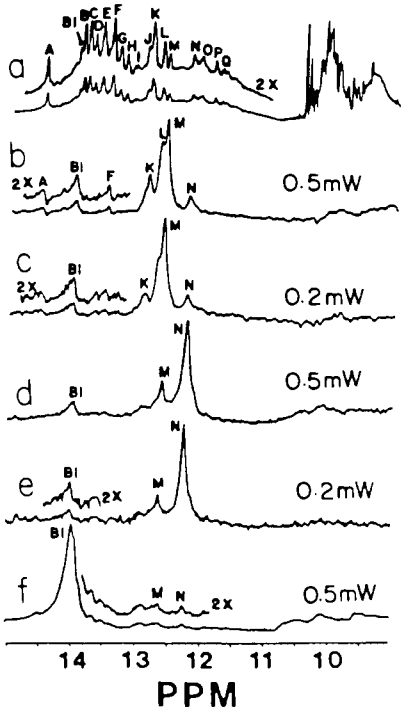

FIGURE 8: 500-MHz proton homonuclear Overhauser difference spectra of yeast 5S rRNA, produced as in Figure 6, for peaks M, N, and B1.

imino proton assignments for two reasons. First, their chemical shifts typically fall in the otherwise uncrowded 10–12.5 ppm region of the ^{1}H NMR spectrum. Second, saturation of either of the two imino protons of a G·U base pair gives a larger NOE (≥15%) than for any other base pair.

Peaks K/L and K/P have been assigned previously to G_2·U_{119} and G_7·U_{114} in the terminal helix. The chemical shifts and strong mutual NOE (Figure 8b–e) between resonances M (11.47 ppm) and N (10.91 ppm) identify them as arising from a third G·U base pair, as noted previously for *T. utilis* 5S RNA (Chen & Marshall, 1986). Moreover, peaks M/N give a small mutual NOE to peak B1, whose broad aromatic NOE (Figure 8f) is characteristic of a G·C pair.

We can thus be confident that resonances M/N represent a third G·U base pair adjacent to a G·C (peak B1). M/N could correspond to U_{81}·G_{99} (both models), G_{67}·U_{111} in the Fox and Woese model, or G_{25}·U_{53} in the Nishikawa and Takemura model. Of these, we can rule out G_{25}·U_{53}, since peaks M/N remain in the spectrum even after RNase T2 removal of primary residues 1–41 (Chen & Marshall, 1986). The simultaneous melting of resonances M/N and B1 at relatively low temperature (40 °C) might appear to favor the assignment of M/N to G_{67}·U_{111} [a terminal G·U, expected to exhibit end fraying (Boyle et al., 1980; Heus et al., 1983)], rather than U_{81}·G_{99}, which is sandwiched between two G·C pairs (G_{79}·C_{100}, G_{82}·C_{98}) and would therefore be expected to melt at a higher temperature. However, we would then expect to observe a fourth G·U pair, and we have not. Therefore, the present results can be explained most easily by assigning peaks M/N to U_{81}·G_{99} in either the Nishikawa and Takemura or the Fox and Woese models, so that the fourth G·U base pair (G_{25}·U_{53} or G_{67}·U_{111}, respectively) exhibits fast exchange with solvent and is therefore NMR invisible.

For the imino hydrogen-bond protons of each of the three G·U base pairs observed in intact yeast 5S rRNA, NOE connectivity to only one of the nearest-neighbor base pairs is observed. More specifically, an Overhauser connection is observed to the neighboring base pair on the 3′-side but not on the 5′-side of the G residue of the G·U pair, in accord with prior similar observations for tRNA (Heus et al., 1983) and prokaryotic 5S RNA (Kime & Moore, 1983; Chang & Marshall, 1986). This one-sided NOE connectivity obviously makes it difficult to extend NOE-inferred base-pair sequences to both sides of a G·U pair. Interestingly, Lee and Marshall (1986a) have observed that irradiation of a G·U pair in 5.8S rRNA does elicit NOE's to base pairs on both sides of the G·U.

Heat-Induced Melting of Yeast 5S Ribosomal RNA. Figure 3 shows 500-MHz proton FT/NMR spectra of yeast 5S rRNA as a function of temperature. As the temperature increases, the rate of chemical exchange of base-pair hydrogen-bond imino protons with water increases, and the imino-proton NMR resonances broaden and lose intensity. The "melting" temperature of a particular base-pair proton resonance thus reflects the thermal stability of that hydrogen bond. Moreover, NMR peaks arising from adjacent secondary base pairs in the same helical segment are expected to melt at similar temperature. Therefore, the base-pair sequence assignment of Table II can now be evaluated according to the experimentally observed melting profiles of Figure 3.

On the basis of Tinoco rules, the thermodynamically weakest segment of the terminal helix should be G_1·C_{120}-G_2·U_{119}-U_3·A_{118}-U_4·A_{117}, corresponding to resonances F, K/L, A, and C, respectively. Consistent with this assignment, the simultaneous melting of peaks A and L, and concurrent decrease in intensity of peaks F, K and C at about 40 °C, is consistent with the continuity of this 4-base-pair segment. Because peak F contains at least three components, peak K contains at least three components, and peak L contains at least two components (see Figure 5), there is no reason to expect that all components will happen to melt at the same temperature; thus, only partial melting of peaks F, K, and C is seen in Figure 3 at 40 °C. The melting of peaks K/P at a higher temperature (50 °C) corroborates its assignment to G_7·U_{114}, which is sandwiched between two G·C base pairs in the terminal helix.

ACKNOWLEDGMENTS

We thank C. E. Cottrell for advice on NMR experiments and Anheuser-Busch Brewery, Inc., Columbus, OH, for providing yeast cells. We also thank L. J. Berliner for use of his Varian E-4 ESR spectrometer.

Registry No. TEMPO-NH_2, 14691-88-4.

REFERENCES

Abdel-Meguid, S.-S., Moore P. B., & Steitz, T. A. (1983) *J. Mol. Biol. 171*, 207–215.

Arter, D. B., & Schmidt, P. G. (1976) *Nucleic Acids Res. 3*, 1437–1447.

Boyle, J., Robillard, G. T., & Kim, S.-H. (1980) *J. Mol. Biol. 139*, 601–625.

Caron, M., & Dugas, H. (1976) *Nucleic Acids Res. 3*, 19–47.

Chang, L.-H., & Marshall, A. G. (1986) *Biochemistry 25*, 3056–3063.

Chen, S.-M., & Marshall, A. G. (1986) *Biochemistry 25*, 5117–5125.

Cramer, F. V. D., Harr, F., & Schlimme, E. (1968) *FEBS Lett. 2*, 136–139.

Fox, G. E., & Woese, C. R. (1975) *Nature (London) 256*, 505–507.

Gralla, J., & Crothers, D. M. (1973) *J. Mol. Biol. 73*, 497–511.

Hansske, F., Sprinzl, M., & Cramer, F. (1974) *Bioorg. Chem. 3*, 367–376.

Hare, D. R., & Reid, B. R. (1982a) *Biochemistry 21*, 1835–1842.

Hare, D. R., & Reid, B. R. (1982b) *Biochemistry 21*, 5129–5131.
Heerschap, A., Haasnoot, C. A. G., & Hilbers, C. W. (1982) *Nucleic Acids Res. 10*, 6981–7000.
Heerschap, A., Haasnoot, C. A. G., & Hilbers, C. W. (1983a) *Nucleic Acids Res. 11*, 4483–4499.
Heerschap, A., Haasnoot, C. A. G., & Hilbers, C. W. (1983b) *Nucleic Acids Res. 11*, 4501–4520.
Heus, H. A., van Kimmenade, J. M. A., van Knippenberg, P. H., Haasnoot, C. A. G., DeBruin, S. H., & Hilbers, C. W. (1983) *J. Mol. Biol. 170*, 393–056.
Hore, J. (1983) *J. Magn. Reson. 55*, 283–300.
Hurd, R. E., & Reid, B. R. (1979a) *Biochemistry 18*, 4005–4011.
Hurd, R. E., & Reid, B. R. (1979b) *Biochemistry 18*, 4017–4024.
Johnston, P. D., & Redfield, A. G. (1981) *Biochemistry 20*, 1147–1156.
Kim, S.-H. (1976) *Prog. Nucleic Acid Res. Mol. Biol. 17*, 182–216.
Kime, M. J., & Moore, P. B (1983) *Biochemistry 22*, 2615–2622.
Kime, M. J., Gewirth, D. T., & Moore P. B. (1984) *Biochemistry 23*, 3559–3568.
Lee, K. M. (1986) Ph.D. Dissertation, The Ohio State University.
Lee, K. M., & Marshall, A. G. (1986a) *Biochemistry 25*, 8245–8252.
Lee, K. M., & Marshall, A. G. (1986b) *Prep. Biochem. 16*, 247–258.
Li, S.-J., & Marshall, A. G. (1986) *Biochemistry 25*, 3673–3682.
Li, S.-J., Wu, J., & Marshall, A. G. (1987) *Biochemistry 26*, 1578–1585.
Luehrsen, K. R., & Fox, G. E. (1981) *Proc. Natl. Acad. Sci. U.S.A. 78*, 2150–2154.
Luoma, G. A., Herring, F. G., & Marshall, A. G. (1982) *Biochemistry 21*, 6591–6598.
Mizuno, H., & Sundaralingam, M. (1978) *Nucleic Acids Res. 5*, 4451–4461.
Morikawa, K., Kawakami, M., & Takemura, S. (1982) *FEBS Lett. 145*, 194–196.
Nishikawa, K., & Takemura, S. (1974a) *J. Biochem. (Tokyo) 76*, 925–934.
Nishikawa, K., & Takemura, S. (1974b) *J. Biochem. (Tokyo) 76*, 935–947.
Nishikawa, K., & Takemura, S. (1974c) *FEBS Lett. 40*, 106–109.
Ofengand, J., & Chen, C. M. (1972) *J. Biol. Chem. 247*, 2049.
RajBhandary, U. L. (1968) *J. Biol. Chem. 243*, 556–564.
Redfield, A. G., Kunz, S. D., & Ralph, E. K. (1975) *J. Magn. Reson. 19*, 114–117.
Reid, B. R. (1981) *Annu. Rev. Biochem. 50*, 969–996.
Reid, B. R., McCollum, L., Ribeiro, N. S., Abbate, J., & Hurd, R. E. (1979) *Biochemistry 18*, 3996–4005.
Rich, A. (1977) *Acc. Chem. Res. 10*, 388–395.
Rordorf, B. R., Kearns, D. R., Kawkins, E., & Chang, S. H. (1976) *Biopolymers 15*, 325–336.
Roy, S., & Redfield, A. G. (1983) *Biochemistry 22*, 1386–1390.
Rubin, G. M. (1975) in *Methods in Cell Biology* (Prescott, D. M., Ed.) Vol. XII, pp 45–64, Academic, New York.
Schimmel, P. R., & Redfield, A. G. (1980) *Annu. Rev. Biophys. Bioeng. 9*, 181–221.
Shulman, R. G., Hilbers, C. W., Kearns, D. R., Reid, B. R., & Wong, Y. P. (1973) *J. Mol. Biol. 78*, 57–69.
Yang, C. H., & Soll, D. (1974) *Proc. Natl. Acad. Sci. U.S.A. 71*, 2838–2842.